

THE SILICON STRIP DETECTOR AT THE MARK II*

ROBERT JACOBSEN, VLADIMIR GOLUBEV,[†] AND VERA LÜTH
*Stanford Linear Accelerator Center,
Stanford University, Stanford, CA 94309, USA*

BRUCE BARNETT, PAUL DAUNCEY, AND JOHN MATTHEWS
Johns Hopkins University, Baltimore, MD 21218, USA

CHRIS ADOLPHSEN, PAT BURCHAT, GIORGIO GRATTA, MARY KING,
LUIS LABARGA, ALAN LITKE, MICHAL TURALA, AND CARLA ZACCARDELLI
*Santa Cruz Institute for Particle Physics,
University of California, Santa Cruz, CA 95064, USA*

ALAN BREAKSTONE, CHRIS KENNEY, AND SHERWOOD PARKER
University of Hawaii, Honolulu, HI 96822, USA

ABSTRACT

We have installed a Silicon Strip Vertex Detector in the MARK II detector at the Stanford Linear Collider. We report on the performance of the detector during a recent test run, including backgrounds, stability and charged particle tracking.

Introduction

We have constructed and installed a Silicon Strip Vertex Detector (SSVD) for the MARK II detector at the Stanford Linear Collider (SLC). It is to be used in the investigation of events containing bottom and charm quarks, where typical impact parameters are 100 to 200 μm .

As we have previously described,^{1,2} the SSVD consists of three layers of silicon detector modules (SDMs) (see Table 1) with 12 modules per layer organized into two detector halves. Each SDM contains a 300 μm thick silicon detector organized as 512 longitudinal strips. The strips are read out through four custom VLSI Microplex³ chips. The material in the active region of each SDM corresponds to 0.47% of a radiation length at normal incidence, including the material of a thin cable underneath the silicon detector.

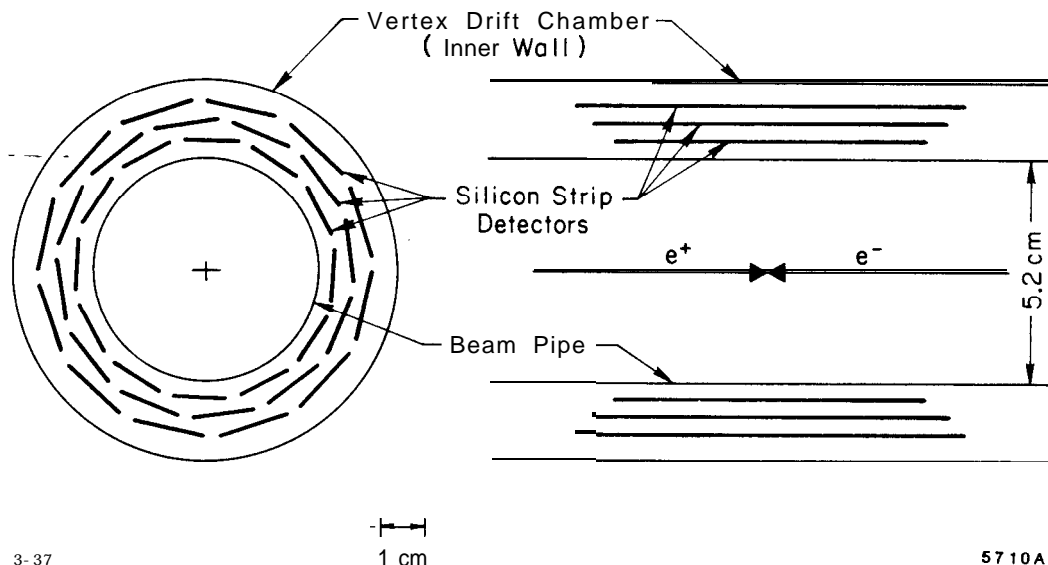
* Work supported by Department of Energy contract DE-AC03-76SF00515.

† Permanent address: Institute of Nuclear Physics, Novosibirsk 630090, USSR.

Invited paper presented at the Vth International Conference on Instrumentation for Colliding Beam Physics, Novosibirsk, USSR, March 15-21, 1990.

Table 1: SSVD dimensions.

Layer	Radius	Active Length	Pitch
1	29 mm	72 mm	25 μm
2	33 mm	82 mm	29 μm
3	37 mm	90 mm	33 μm

**Figure 1:** Overall layout of the Silicon Strip Vertex Detector.

The SDMs are held between slotted aluminum endplates by spring loaded fixtures. The endplates are connected by inner and outer shells of 380 μm thick beryllium and are attached to the beampipe by a three-point mount. The split between the two detector halves is oriented approximately horizontally. The beampipe is made from 430 μm aluminum with a 25 μm copper liner. The active regions in each layer occupy at least 85% of the circumference and are staggered for best coverage of tracks coming from the origin (see Fig. 1). The SDMs extend to $|\cos\theta| \leq 0.78$. Within this, half of all tracks from the origin cross three SDMs and half of them cross two SDMs.

The SDMs were assembled into their holders under an optical microscope to ensure correct alignment. They were then surveyed using a collimated x-ray beam^{4,5} to determine their exact orientation within the SSVD reference frame. Simultaneously the twist and bowing of each of the 36 SDMs were measured and the gain of each channel determined. We wanted to measure accurately enough to be able to calculate the position of any point on the detector with a spatial accuracy of 5 μm . This initial alignment survey provides an important starting point for later track-based alignment, as the number of clean tracks from Z^0 decays is expected

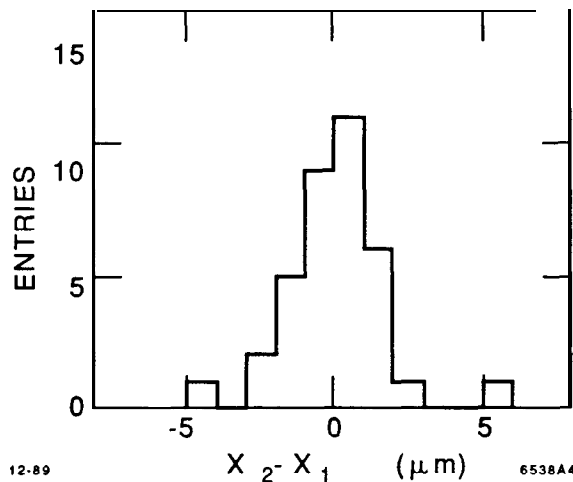


Figure 2: Difference between two sets of measurements of detector position. The SSVD was removed from the beampipe and remounted between measurements.

to be small, Comparison of two measurements of the detector give some confidence that this accuracy has been achieved (see Fig. 2).

Installation and Running Experience

One SDM **module** failed during insertion of the SSVD and beampipe into the center of the MARK II detector. We believe that an intermittently open trace developed in the custom thin cable leading from the SDM. We were unable to fix it and have disabled readout of the module. In addition to the 512 unusable strips in this module, there are approximately 200 strips which fail calibration tests or are known to be bad from prior x-ray tests. This leaves about 17,700 good strips (96%).

During January 1990, the MARK II recorded a total of 37 Z^0 decays. These included a decay to a pair of τ leptons, two wide-angle e^+e^- pairs and 34 hadronic decays. Tracking in the main drift chamber found a total of 689 tracks, of which 355 passed quality and fiducial cuts for the SSVD active area. Of these, 220 had momenta exceeding 1 GeV/c.

This run was the first with detector components at small radius and new backgrounds were seen.⁶ Occupancy in the SSVD improved over the course of the run. Background levels after initial startup were not a problem for the SSVD when the rest of the detector was able to take data. This is because of the fine spatial segmentation of the silicon strips and because energy depositions below about 10 keV are suppressed by thresholds in the readout.

In order to monitor the position of the SSVD with respect to the Drift Chamber Vertex Detector (DCVD)⁷ a capacitive displacement-measuring system was developed.⁷ Briefly, it consists of 20 capacitive sensors, of which 14 are used to measure all degrees of freedom of each half of the detector. Measurements using

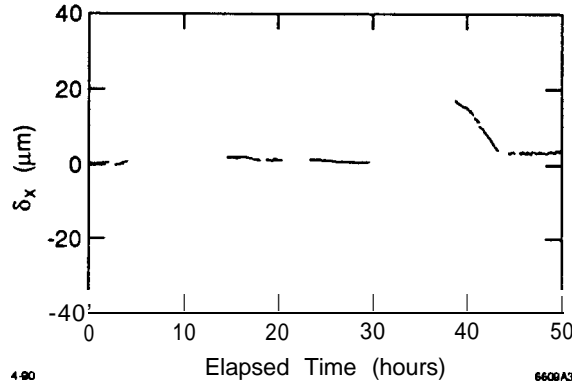


Figure 3: Changes in the X position of the SSVD with respect to the DCVD during the test run. The other degrees of freedom show motions of similar magnitude.

the gap directly were expected to have an accuracy of about $2 \mu\text{m}$. Measurements of transverse position, which involves the capacitance change due to change in the overlap of a sensor and a ground pad, were expected to have a repeatability of $20 \mu\text{m}$. Measured motions during data running were negligible. Figure 3 shows a typical sensor readout over a two-day span. The motion starting near 39 hours is an example of movements seen when the MARK II solenoid is turned on and off.

Tracking and Alignment

Charged particle track reconstruction starts in the Central Drift Chamber (CDC).⁹ These tracks are then refit using information from the DCVD. The track is then extrapolated **into** the SSVD volume and all possible combinations of clusters within a small road are tried. The best match of the track to three clusters is used if it has a χ^2/DOF less than a fixed cut. If not, matches to two, then one cluster are attempted. The error matrix used in the χ^2 calculation includes explicit multiple scattering in each of the material layers of the SSVD and the track parameter errors provided by the CDC and DCVD. Backgrounds in these detectors and/or closely spaced tracks occasionally adversely affected their ability to find and fit tracks.

To examine the internal resolution and alignment of the SSVD we calculate a quantity A for each track matched to three clusters. The middle track intercept is defined as the point where a line drawn from the cluster in the inner layer to the cluster in the outer layer crosses the middle layer. Delta is defined as the signed distance from this middle track intercept to the cluster in the middle layer. The longitudinal coordinate z of the clusters is assumed to be where the track crosses the detector layers. The distance is computed in the xy plane. Figure 4 shows mean Δ/σ_Δ , where σ_Δ includes multiple scattering and the expected SDM resolution, as a function of the ϕ angle around the detector. Two regions show larger values. Closer examination of the data in those regions indicates that 4 SDMs appear to have moved by 10 to $20 \mu\text{m}$ since the x-ray alignment data was taken. With additional

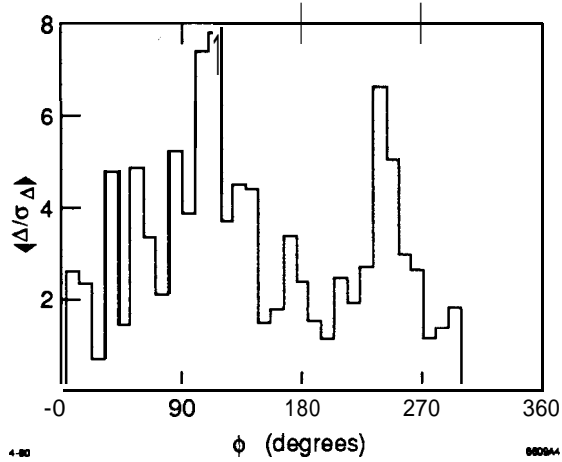


Figure 4: Mean Δ/σ_{Δ} as a function of ϕ . Note the large values from 90° to 160° and from 240° to 280° . From 320° to 360° is zero due to the nonfunctional module and the overlap of the two halves of the SSVD.

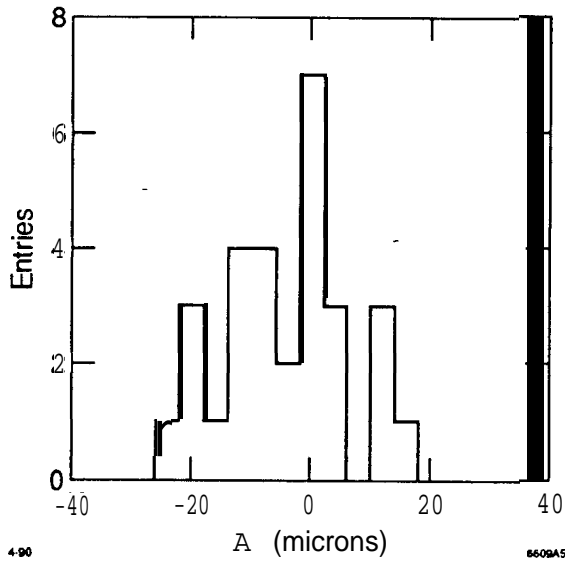


Figure 5: The distribution of A for tracks with transverse momentum greater than $1 \text{ GeV}/c$. The regions pointed out in the caption of Fig. 4 are not included. The RMS value is $10.5 \mu\text{m}$.

tracks we expect to be able to refit for the alignment constants of these modules. Omitting these regions, Fig. 5 shows the A distribution for tracks with transverse momentum greater than $1 \text{ GeV}/c$. (Tracks in these regions are included in all other analyses described here.) The RMS value is $10.5 \mu\text{m}$ for 27 tracks.

A Monte Carlo simulation of the A distribution starts with estimated detector spatial resolutions¹⁰ of $5, 6$ and $6.6 \mu\text{m}$ for the inner through outer layers, respectively. For tracks perpendicular to the detectors this would correspond to an expected RMS of $7.3 \mu\text{m}$ before multiple scattering. Corrections are then applied

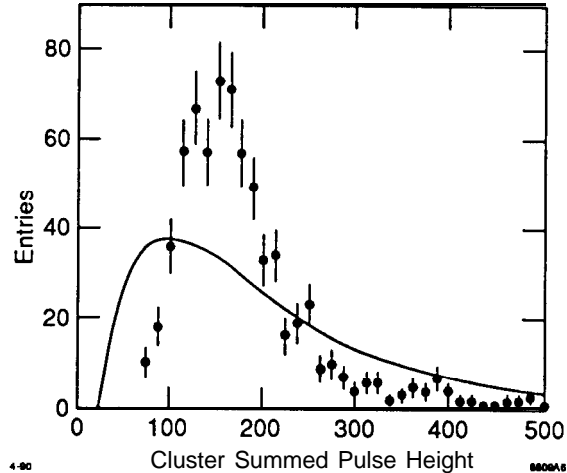


Figure 6: Total pulse height in cluster. The solid line is from random beam crossings. The points are from successfully matched tracks in Z^0 decay events.

for tracks not perpendicularly incident on the detectors and multiple scattering. With only these effects, the RMS value of A is expected to be $9.1 \mu\text{m}$. Addition of mistracking as modeled by the full MARK II Monte Carlo raises this to $9.7 \mu\text{m}$. Finally, mixing background random events with the Monte-Carlo-simulated Z^0 decays and thus adding several percent occupancy raises the expected A RMS value to $10.2 \mu\text{m}$.

To determine the cluster finding efficiency of the detector, tracks were selected with momenta greater than $1 \text{ GeV}/c$, no other tracks within 0.1 radian and satisfying geometric cuts to ensure they were inside the SSVD active region. All possible combinations of two layers were then examined. If clusters in those two layers had been matched onto the track, that track was considered well tracked and the location where it crossed the remaining layer was examined. There were 32 such occurrences, with the third hit being outside the active area in 12, and having a found cluster within four strips in 18. There was no cluster found in the two remaining cases, although both had readout strips in the vicinity, due to the presence of strips marked as bad. This is consistent with the detector being 100% efficient in good regions.

Figure 6 shows the distribution of pulse height from clusters matched onto tracks and from clusters from random beam crossings. Similarly, Fig. 7 shows the distribution of cluster widths. Some separation can be made between signal and background clusters but the improvement is small. The noise in a single channel is approximately 8 counts and in the sum of three adjacent channels is approximately 12 counts? As the readout electronics searches for signals in overlapping regions three strips wide, the most probable signal of 165 counts gives an effective signal-to-noise ratio of 14.

◊ The electronics creates negative correlations between adjacent channels which reduce this sum below the $8\sqrt{3}$ normally expected.

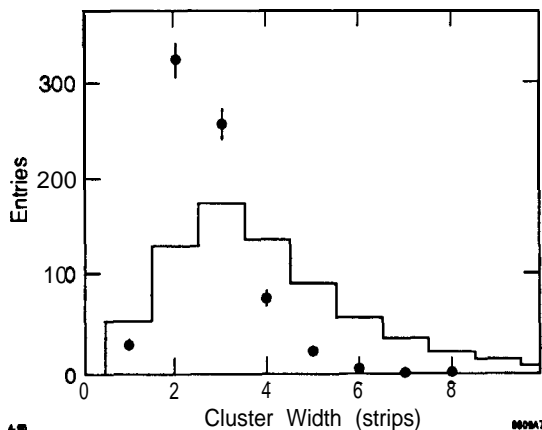


Figure 7: Cluster width. The solid line is from random beam crossings. The points are from successfully matched tracks in Z^0 decay events. The mean value for matched tracks is 2.7 strips.

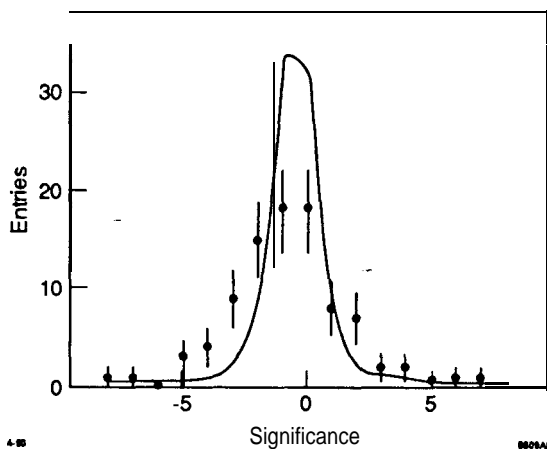


Figure 8: Impact parameter significance for tracks with expected impact parameter resolution better than $40 \mu\text{m}$. The IP used is from the average of all events. The solid line is Monte Carlo data and the points with error bars are from Z^0 decays.

We find the interaction point (IP) in each event by fitting all tracks passing fiducial and quality cuts to a single point. The track with the largest χ^2 contribution is removed and successive iterations performed until the χ^2/DOF decreases by less than 1 when the track with the largest contribution to χ^2 is removed. Monte Carlo studies using a simulation of our current tracking indicate that the RMS error in estimating the IP is $120 \mu\text{m}$ in the core of the distribution, with tails extending to much larger values. Note that this is dominated by inclusion of tracks not originating at the true IP, as the tracking resolution would only lead to an RMS of $60 \mu\text{m}$. The same analysis on the 34 Z^0 hadronic decays gives an RMS scatter of $125 \mu\text{m}$ in x and in y after discarding 4 events as lying in the tail of the distribution.

Using the mean of all primary vertices found with this method as a best estimate of the true IP position, we plot in Fig. 8 the significance of the impact parameter

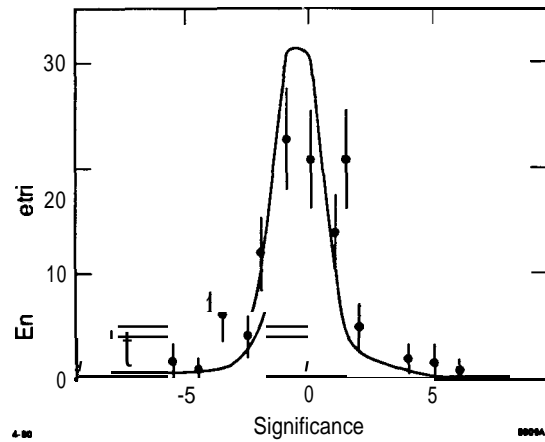


Figure 9: Impact parameter significance for tracks with expected impact parameter resolution better than $40 \mu\text{m}$. The IP used has been found in each event. The solid line is Monte Carlo data and the points with error bars are from Z^0 decays.

of the tracks with respect to this point. The significance is defined as the measured impact parameter divided by the expected error, including both the impact parameter error for the track and the error ellipse for the IP position. The track error includes detector resolutions and calculated multiple scattering. Figure 8 shows this for all tracks with impact parameter resolution calculated to be better than $40 \mu\text{m}$. This cut value was chosen for maximum sensitivity to tracking errors on the order of $40 \mu\text{m}$. The mean impact parameter resolution for this set of tracks is $25 \mu\text{m}$.

Motion of the IP, if present, would broaden the observed distribution. The SLC control system provides MARK II with beam position monitor information and magnet values on a regular basis. Analysis of this information is not yet complete, but it appears certain that motion of the IP is at or below the $40 \mu\text{m}$ level. To reduce any effect of beam motion, we plot in Fig. 9 the impact parameter significance with respect to the primary vertex found in each event. Tracking errors on the scale of $40 \mu\text{m}$ would significantly broaden this distribution.

Conclusion

The Silicon Strip Vertex Detector at the MARK II is successfully taking data. We have shown that a silicon detector with integrated readout can be made to work 30 mm from colliding beams, that the problem of alignment is solvable, and that this type of detector can be producing measurements to better than $40 \mu\text{m}$ resolution with only a minimal amount of data.

We expect to do B physics using this detector with the data sample from this summer's SLC running.

Acknowledgments

We would like to thank David Drewer, David Hutchinson, Michel Lateur, and Andreas Schwarz for their assistance in the construction of this detector and its support systems.

References

1. A. Litke et al., *Nucl. Instrum. Methods* **A265** (1988) 93.
2. C. Adolphsen et al., *IEEE Trans. Nucl. Sci.* NS-35 (1988) 424.
3. J. T. Walker et al., *Nucl. Instrum. Methods* **A226** (1984) 200.
4. C. Adolphsen et al., *Nucl. Instrum. Methods* **A288** (1990) 257-264.
5. G. Anzivino et al., *Nucl. Instrum. Methods* **A243** (1986) 153.
6. R. Jacobsen et al, "Detector Background Conditions at the SLC," *Proc. Vth Int. Conj. on Instrumentation for Colliding Beam Physics*, Novosibirsk, 1990.
7. J. Jaros, "Performance of the MARK II Drift Chamber Vertex Detector," *Proc. Vth Int. Conj. on Instrumentation for Colliding Beam Physics*, Novosibirsk, 1990.
8. A. Breakstone et al., *Nucl. Instrum. Methods* **A281** (1989) 453-461.
9. G. Abrams et al, *Nucl. Instrum. Methods* **A281** (1989) 55-80.
10. C. Adolphsen et al., *Nucl. Instrum. Methods* **A253** (1987).